Heliyon 9 (2023) e13707

Contents lists available at ScienceDirect

Heliyon

journal homepage: www.cell.com/heliyon

Research article

# Cytoskeleton regulator RNA expression on cancer-associated fibroblasts is associated with prognosis and immunotherapy response in bladder cancer

Yucai Wu [a,b,c,d,1], Yangyang Xu [a,b,c,d,1], Shiming He [a,b,c,d], Yifan Li [e], Ninghan Feng [f,*], Jian Fan [a,b,c,d,**], Yanqing Gong [a,b,c,d], Xuesong Li [a,b,c,d,***], Liqun Zhou [a,b,c,d,****]

[a] *Department of Urology, Peking University First Hospital, Beijing, China*
[b] *Institute of Urology, Peking University, Beijing, China*
[c] *National Urological Cancer Center, Beijing, China*
[d] *Urogenital Diseases (Male) Molecular Diagnosis and Treatment Center, Peking University, Beijing, China*
[e] *Department of Urology, The Affiliated Hospital of Yangzhou University, Yangzhou University, Jiangsu, China*
[f] *Wuxi No 2 People's Hospital, Jiangsu, China*

ARTICLE INFO

*Keywords:*
Bladder cancer
*CYTOR*
Survival
Immune infiltration
Immunotherapy

ABSTRACT

*Background:* Dysregulation of long noncoding RNAs (lncRNAs) has been reported to be associated with multiple tumors where they act as tumor suppressors or accelerators. The lncRNA *CYTOR* was identified as an oncogene involved in many cancers, such as gastric cancer, colorectal cancer, hepatocellular carcinoma, and renal cell carcinoma. However, the role of *CYTOR* in bladder cancer (BCa) has rarely been reported.

*Methods:* Using cancer datasets from The Cancer Genome Atlas (TCGA) program, we analyzed the association between *CYTOR* expression and prognostic value, oncogenic pathways, antitumor immunity and immunotherapy response in BCa. The influence of *CYTOR* on the immune infiltration pattern in the urothelial carcinoma microenvironment was further verified in our dataset. Single-cell analysis revealed the role of *CYTOR* in the tumor microenvironment (TME) of BCa. Finally, we evaluated the expression of *CYTOR* in BCa in the Peking University First Hospital (PKU–BCa) dataset and its correlation with the malignant phenotype of BCa *in vitro* and *in vivo*.

*Results:* The results indicated that *CYTOR* was highly expressed in multiple cancer samples, including BCa, and increased *CYTOR* expression contributed to poor overall survival (OS). Additionally, elevated *CYTOR* expression was significantly correlated with clinicopathological

*Abbreviations:* LncRNAs, Long non-coding RNAs; BCa, Bladder cancer; TCGA, The Cancer Genome Atlas; TME, Tumor microenvironment; OS, Overall survival; EMT, Epithelial mesenchymal transformation; PD-1, Programmed cell death-1; PD-L1, Programmed death ligand 1; MIBC, Muscle-invasive bladder cancer; CYTOR, Cytoskeleton regulator RNA; UTUC, Upper-tract urothelial carcinoma; UMI, Unique molecular identifier; PCA, Principal component analysis; CIBERSOFT, Cell-type Identification By Estimating Relative Subsets Of RNA Transcripts; RT-qPCR, Reverse transcription-quantitative polymerase chain reaction; CAFs, Cancer-associated fibroblasts.

* Corresponding authors. Wuxi No 2 People's Hospital, NO.68, Zhongshan Road, Wuxi, Jiangsu 214002, China.
** Corresponding author. Department of Urology, Peking University First Hospital, NO.8, Xishiku Street, Xicheng, Beijing 100034, China.
*** Corresponding authors. Department of Urology, Peking University First Hospital, NO.8, Xishiku Street, Xicheng, Beijing 100034, China.
**** Corresponding author. Department of Urology, Peking University First Hospital, NO.8, Xishiku Street, Xicheng, Beijing 100034, China.
*E-mail addresses:* n.feng@njmu.edu.cn (N. Feng), JFan_bio@163.com (J. Fan), pineneedle@sina.com (X. Li), zhoulqmail@sina.com (L. Zhou).
[1] Contributed equally.

https://doi.org/10.1016/j.heliyon.2023.e13707
Received 22 November 2022; Received in revised form 1 January 2023; Accepted 8 February 2023
Available online 13 February 2023

features of BCa, such as female sex, advanced TNM stage, high histological grade and non-papillary subtype. Functional characterization revealed that *CYTOR* may be involved in immune-related pathways and the epithelial mesenchymal transformation (EMT) process. Moreover, *CYTOR* had a significant association with infiltrating immune cells, including M2 macrophages and regulatory T cells (Tregs). *CYTOR* facilitates the crosstalk between cancer-associated fibroblasts (CAFs) and macrophages, and mediates M2 polarization of macrophages. Correlation analysis revealed a positive correlation between *CYTOR* expression and programmed cell death-1 (*PD-1*)/programmed death ligand 1 (*PD-L1*)/expression and other targets for specific immunotherapy in BCa, which are recognized to predict the efficacy of immunotherapy.
*Conclusions:* These results suggest that *CYTOR* serves as a potential biomarker for predicting survival outcome, TME cell infiltration characteristics and immunotherapy response in BCa.

## 1. Introduction

Bladder cancer (BCa) is the most common malignant tumor within the urogenital system and accounts for 170,000 deaths worldwide annually [1]. Although surgical resection is feasible for many patients after diagnosis of the tumor, the overall outcome of treatment for muscle-invasive bladder cancer (MIBC) and metastatic bladder cancer remains unsatisfactory [2]. Platinum-based chemotherapy and *anti*-PD-1/PD-L1 immunotherapy have been shown to exert a prodigious antitumor effect on metastatic bladder cancer for the past three decades [2]. However, drug resistance has also received greater experimental attention. In recent years, innovations and applications of sequencing technologies have deepened our understanding of bladder cancer pathogenesis. Therefore, the development of new therapeutic approaches against commonly expressed molecular targets or potential markers has become a promising direction to improve clinical treatment strategies and patient prognosis of BCa.

LncRNAs are a class of nonprotein-coding molecules over 200 nucleotides in length that are involved in many physiological and pathological processes of tumors [3,4]. Alterations in lncRNA expression and mutations are closely related to tumor occurrence, development, metastasis and suppression, which suggests that lncRNAs could be novel biomarkers and therapeutic targets for cancer [5]. Increasing evidence also suggests that lncRNAs are involved in the chemotherapy response and prognosis of BCa [6,7]. Recent studies have also shown that lncRNAs play fundamental roles in regulating genes encoding products involved in cancer immunity, which suggests that lncRNAs have potential in evaluating tumor immune cell infiltration [8–10]. Cytoskeleton regulator RNA (*CYTOR*), also known as *LINC00152*, is a lncRNA that has been reported to be elevated in several tumors and correlated with poor prognosis [4,11–14]. However, the role of *CYTOR* in the development, progression and treatment of BCa has not been entirely elucidated.

Herein, using TCGA and PKU datasets, we evaluated the expression of *CYTOR* in BCa and its correlation with clinicopathologic features to reveal its biological effects on cancer progression and prognosis. Our results indicated that *CYTOR* may serve as a potential biomarker predicting prognosis and immunotherapy effects in BCa.

## 2. Methods

### 2.1. Clinical samples and study approval

A total of 24 pairs of tumor tissues and adjacent normal urothelium from patients with BCa who underwent surgery were obtained from Peking University First Hospital (PKU–BCa dataset) and used to create a cDNA library of BCa. In addition, 29 fresh samples of upper-tract urothelial carcinoma (UTUC) were obtained from Peking University First Hospital after ureterectomy or radical nephroureterectomy between January 2015 and December 2019 for the RNA sequencing assay (PKU-UTUC dataset). All experiments were conducted with the approval of the Biomedical Research Ethics Committee of Peking University First Hospital (Beijing, China). Written informed consent was obtained from all participants before sample collection.

### 2.2. RNA sequencing assay

The RNA-Seq experiments were performed by Biotechnology Corporation (Shanghai, China). Briefly, total RNA from $1 \times 10^6$ cells was extracted using TRIzol reagent (Invitrogen). Library preparation and transcriptome sequencing on an Illumina HiSeq 2000 platform were performed, and 100-bp paired-end reads were generated. The read numbers mapped to each gene were counted by HTSeq v0.6.0, and the fragments per kilobase of transcript per million fragments mapped (FPKM) of each gene were calculated.

### 2.3. Data acquisition

The gene expression matrix (FPKM and count format) was obtained from the TCGA website (https://portal.gdc.cancer.gov/), including a set of 19 normal samples and 411 BCa samples. The matrix of lncRNA expression was extracted separately according to the genomic annotations using the Gencode (GENCODE v 26) GTF file and normalized. LncRNAs with “zero” expression in 90% of BCa patients were excluded. Clinical data of these samples were downloaded from the UCSC Xena website (https://xena.ucsc.edu/). To analyze the correlation of the lncRNA expression with the prognosis of BCa patients, we selected 405 patients with available clinical

information. The stromal score and immune score of BCa were calculated by applying the ESTIMATE algorithm and downloaded from https://bioinformatics.mdanderson.org/estimate/index.html [15]. The 'HALLMARK_EPITHELIAL_MESENCHYMAL_TRANSITION' gene list, including 200 genes that participate in EMT, was downloaded from the Gene Set Enrichment Analysis (GSEA) database (http://software.broadinstitute.org/gsea/in-dex.jsp) [16]. Single-cell RNA sequencing data of BCa tissues, including eight primary bladder tumor tissues and three adjacent normal urothelium, were obtained from GSA-Human under the accession code HRA000212.

### 2.4. Raw data of scRNA-Seq processing and quality control

Cell Ranger (version 7.0.0) was used to process the raw data and map reads to the transcriptome as per default parameters. These procedures produced a raw unique molecular identifier (UMI) count matrix, which was converted into a Seurat object by the R package Seurat 29 (version 4.2.0). Cells with UMI numbers <1000 or with over 10% mitochondrial-derived UMI counts were considered low-quality cells and were removed. To eliminate potential doublets, single cells with over 6000 genes detected were also filtered out. Finally, 71,766 single cells remained, and they were used in downstream analysis.

Principal component analysis (PCA) was conducted on an integrated data matrix to reduce the dimensionality of the scRNA-Seq dataset. Downstream analysis was performed on the top 75PCs using the ElbowPlot function of Seurat. The main cell clusters were identified by Seurat, with resolution set as default (res = 1). Then, they were visualized with 2D tSNE. Conventional markers were used to classify every cell into a known biological cell cluster. Consequently, 71,766 cells were clustered into eight major cell types.

### 2.5. Quantification of immune cell infiltration

Cell-type Identification By Estimating Relative Subsets Of RNA Transcripts (CIBERSOFT) is a gene-based deconvolution algorithm that can infer 22 human immune cell types and uses the characteristics of 547 marker genes to quantify the relative score of each cell type (http://cibersort.stanford.edu) [17]. By this algorithm, we can estimate the immune cells contained in the input sample based on a known training set that contains the gene expression characteristics of different immune cells.

### 2.6. Pathway enrichment analysis

To explore the potential functions of *CYTOR* in BCa, GSEA was conducted to assess whether a predefined set of genes showed statistically significant, concordant differences according to the expression level of *CYTOR* by GSEA software. The gene sets of "c2. cup. kegg.v6.2. symbols.gmt" from the molecular signatures database were analyzed. The significance threshold of false discovery rate (FDR) for significantly enriched biological processes and pathways was set at 0.05.

### 2.7. Cell culture

The cell lines SV-HUC-1, UM-UC-3, EJ, BIU87, 5637, T24, J82 and SW780 were used in this study. The normal human urinary tract epithelial SV-HUC-1 cell line was cultured in F–12K medium (Gibco; Thermo Fisher Scientific, Inc.). T24, SW780, UM-UC-3 and J82 cells were cultured in Dulbecco's modified Eagle's medium (Gibco; Thermo Fisher Scientific, Inc.), while EJ, BIU87 and 5637 cells were cultured in RPMI-1640 (Gibco; Thermo Fisher Scientific, Inc.). All media contained 10% fetal bovine serum (Gibco; Thermo Fisher Scientific, Inc.) and 1% penicillin G-streptomycin (Sigma-Aldrich; Merck KGaA). The cell cultures were maintained as a monolayer culture in a humidified atmosphere containing 5% $CO_2$ at 37 °C.

### 2.8. Reverse transcription-quantitative polymerase chain reaction (RT-qPCR)

RT-qPCR was performed as previously reported [18]. Briefly, total RNA was first extracted from cell lines or tissues and reversed transcribed into cDNA according to the manufacturer's protocols (TIANGEN). RT-qPCR was performed in 200 μl tubes (NEST Biotechnology, Cat. No.401001) using the 7500 Fluorescent Quantitative PCR System (Applied Biosystems; Thermo Fisher Scientific, Inc.). The primer sequences are listed in Table S1. The reaction program was set as follows: 94 °C for 30 s, then 40 cycles at 94 °C for 5 s and at 60 °C for 30 s. All experiments were repeated at least three times.

### 2.9. Plasmid construction and lentivirus infection

The *CYTOR* short hairpin RNA (shRNA) oligonucleotides were designed by an online shRNA designer tool (https://portals.broadinstitute.org/gpp/public/), and then were inserted into pLKO.1-TRC vector (Addgene, Watertown, MA, USA). Lentivirus was produced in HEK-293 T cells using a three-vector system, which contained the targeted vectors, the packaging construct (psPAX2), and the envelope plasmid (pMD2G) in a 4:3:1 ratio, respectively. Stable knockdown cell lines were selected for 2 weeks by treatment with 1.0 μg/mL of puromycin. The interference efficiency was detected by RT-qPCR.

### 2.10. Transwell migration and invasion assay

For the Transwell migration assay, 40,000 cells were seeded into the upper chambers (24-well insert, Corning). The upper chambers were filled with 300 μL serum-free PRIM-1640 medium, while the lower chambers contained 700 μL PRIM-1640 medium

with 10% fetal bovine serum. For the Transwell invasion assay, 25,000 cells were plated into the upper chambers (24-well insert, Corning) coated with Matrigel (diluted 1:8 in PBS; product #354234; Corning, USA). After 24 h, the cells under the surface of the lower chamber were fixed with 4% paraformaldehyde for 20 min, followed by a 1 h 0.5% crystal violet staining.

### 2.11. Mouse model experiments

Animal experiments were performed in accordance with the N IH Guidelines for the Care and Use of Laboratory Animals and were approved by the Review Board of Peking University First Hospital (Beijing, China). Four-week-old male BALB/c nude mice were purchased from Vitalriver (Beijing, China). Then, approximately $5 \times 10^6$ T24-*CYTOR*-sh/T24 -sh-NC cells suspended in 100 μL PBS were mixed with Matrigel (1:1, Product #354234, Corning Inc., NY, USA), and the mixture was injected subcutaneously into the right flank of five-week-old BALB/c nude mice.

### 2.12. Statistical analysis

The chi-square test or Fisher's exact test was conducted to measure the correlation between *CYTOR* expression and clinical data. Spearman's correlation coefficients were computed to investigate the potential relationship between two groups. Both univariable and multivariable Cox regression analyses were performed using the R package 'survival'. The Kaplan–Meier survival curve with log-rank test was drawn to demonstrate the relationship between *CYTOR* expression and OS by the R package 'survival'. The Wilcoxon rank-sum test is a nonparametric statistical test mainly utilized for comparing two groups. All reported p values are from two-sided statistical tests, and differences with $p \leq 0.05$ were considered significant. All analyses were performed in SPSS version 25.0 (SPSS Inc., Chicago,

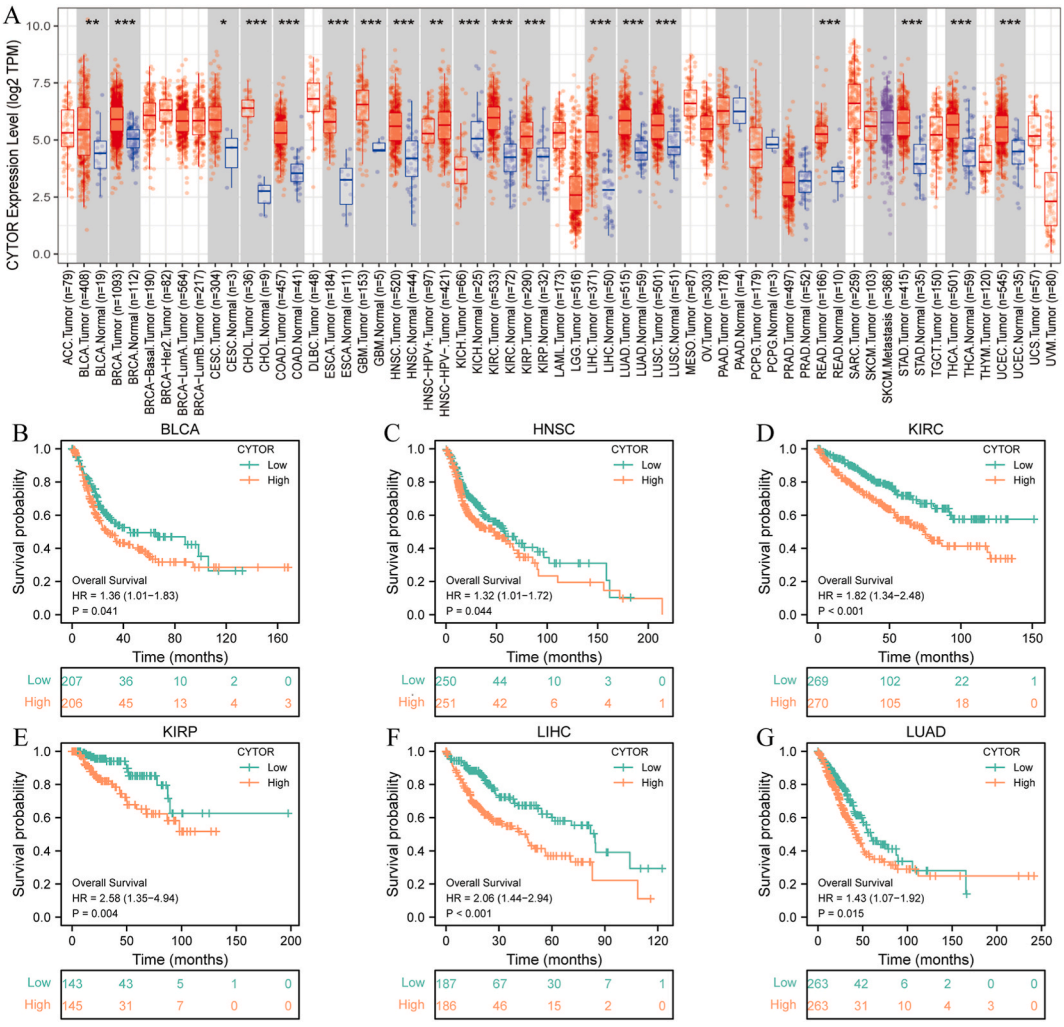


**Fig. 1.** Expression and prognostic significance of *CYTOR* in multiple tumors. (A) The mRNA level of *CYTOR* in multiple tumors. (B–G) *CYTOR* expression was related to the OS in BLCA (B), HNSC (C), KIRC (D), KIRP(E), LIHC (F) and LUAD (G). *p < 0.05, **p < 0.01, ***p < 0.001.

IL, USA) or R version 3.5.2 (http://www.r-project.org/).

## 3. Results

### 3.1. Prognostic significance of CYTOR across cancers

We first used the web platform TIMER2.0 to determine *CYTOR* expression in multiple cancers [19]. The results demonstrated that *CYTOR* expression was significantly elevated in BCa, breast cancer (BRCA), cervical squamous cell carcinoma and endocervical adenocarcinoma (CESC), cholangiocarcinoma (CHOL), colon adenocarcinoma (COAD), esophageal carcinoma (ESCA), glioblastoma multiforme (GBM), head and neck squamous cell carcinoma (HNSC), kidney renal clear cell carcinoma (KIRC), kidney renal papillary cell carcinoma (KIRP), liver hepatocellular carcinoma (LIHC), lung adenocarcinoma (LUAD), lung squamous cell carcinoma (LUSC), rectum adenocarcinoma (READ), stomach adenocarcinoma (STAD), thyroid carcinoma (THCA), and uterine corpus endometrial carcinoma (UCEC) samples but decreased in kidney chromophobe (KICH) samples, compared with the associated normal tissues (Fig. 1A). Our main finding is that *CYTOR* is significantly overexpressed in most tumors.

Next, we explored the correlation between *CYTOR* and OS among the tumors mentioned above. We found that multiple cancer types exhibited a significant association between *CYTOR* expression and OS, including BCa, HNSC, KIRC, KIRP, LIHC and LUAD, and high *CYTOR* expression tended to predict a poor outcome in most tumors (Fig. 1B–G). In addition, high *CYTOR* expression was correlated with high pathological stage in malignancies (Figure S1). The expression pattern of *CYTOR* suggests that it may act as an oncogene during tumor progression.

### 3.2. Correlation between CYTOR expression and clinicopathological features of BCa

Next, we mainly explored the role of *CYTOR* expression in the pathogenesis of BCa. In a total of 430 samples, *CYTOR* expression was significantly elevated in 411 tumor samples compared to 19 adjacent tissue samples (Fig. 2A). Meanwhile, we found significantly higher *CYTOR* expression in tumor samples with advanced pathologic T stage (Fig. 2B) and histological grade (Fig. 2C). In addition, the expression of *CYTOR* was higher in dead patients than in living patients (Fig. 2D), and patients with high *CYTOR* expression were prone to local recurrence (Fig. 2E). To determine the diagnostic value of *CYTOR* expression in BCa, receiver operator characteristic (ROC)

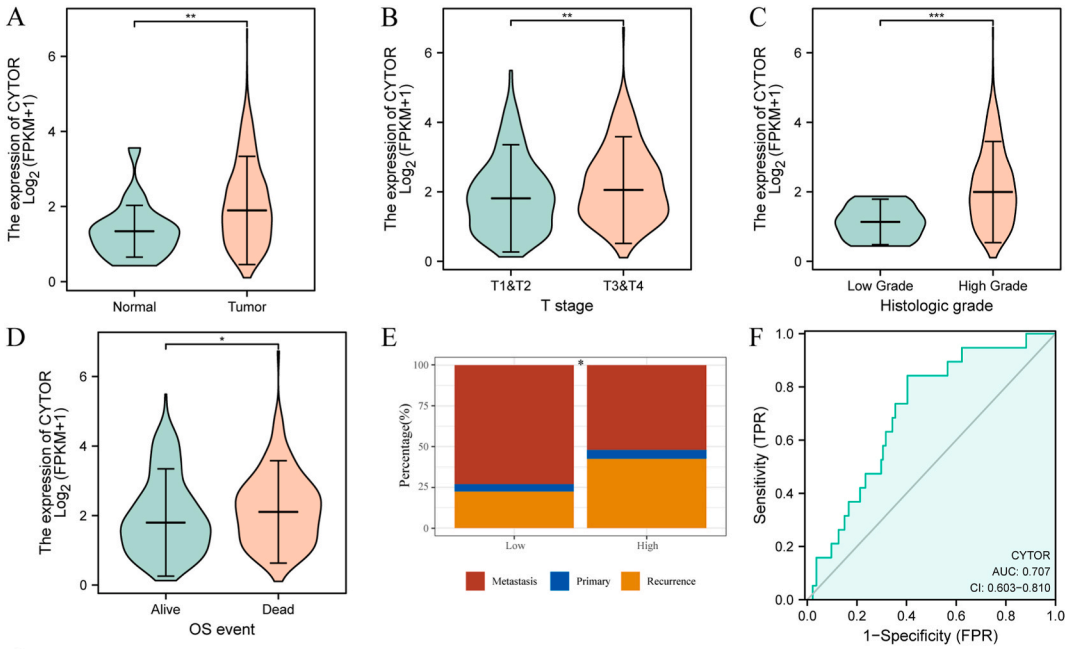


G

| Marker | Cutoff value | Sensitivity | Specificity | PPV | NPV | Youden index |
|---|---|---|---|---|---|---|
| CYTOR | 1.662 | 0.842 | 0.597 | 0.087 | 0.988 | 0.439 |

**Fig. 2.** Enhanced *CYTOR* expression was involved in the poor prognosis of BCa. (A) The mRNA level of *CYTOR* in BCa tumor tissues and adjacent normal urothelium. (B–E) High *CYTOR* expression was related to advanced T stage (B), advanced histological grade (C), increased mortality (D) and common local recurrence (E). (F) ROC curve of *CYTOR* expression to predict patients with BCa. (G) Diagnostic value of *CYTOR* for differentiating between BCa and control groups. PPV, positive predictive value; NPV, negative predictive value; *p < 0.05, **p < 0.01, ***p < 0.001.

curves were generated. The area under the curve (AUC) value for *CYTOR* expression to discriminate between normal cases and tumor cases reached as high as 0.707 (Fig. 2F and 95% CI: 0.603–0.810, $p < 0.01$), and the sensitivity and specificity were 0.842 and 0.597, respectively. To understand the association between *CYTOR* expression and clinicopathological features, we performed a correlation analysis. The results showed that high *CYTOR* expression was significantly associated with female sex ($p = 0.019$), advanced pathologic stage ($p < 0.001$) and histologic grade ($p = 0.002$), and the non-papillary subtype of BCa ($p < 0.001$) (Table 1). However, univariate analysis followed by multivariate analysis showed that *CYTOR* expression was not an independent risk factor for OS in BCa patients (Table 2).

### 3.3. Pathway enrichment analysis of CYTOR in BCa

To study the potential molecular mechanism of *CYTOR* in BCa, coexpressed genes of *CYTOR* in TCGA were selected for enrichment analysis. The results of GO enrichment analysis showed that *CYTOR* was associated with immune-related pathways, such as T cell activation, leukocyte cell–cell adhesion, regulation of T cell activation and regulation of leukocyte cell–cell adhesion (Fig. 3A). KEGG pathway analysis also showed that most coexpressed genes were involved in the immune system, including the chemokine signaling pathway, hematopoietic cell lineage, and Th17 cell differentiation (Fig. 3B). Moreover, GSEA of coexpressed *CYTOR* genes showed enrichment of monocyte chemotaxis ($p < 0.001$, Fig. 3C). Interestingly, genes involved in extracellular structure organization and extracellular matrix organization were also enriched by GO analysis, which indicated that *CYTOR* may be involved in the EMT process in BCa (Fig. 3A). EMT has been confirmed to play a key role in tumorigenesis, invasion and metastasis. We observed a marked positive correlation between the expression levels of *CYTOR* and EMT-related genes (Fig. 3D). In addition, elevated expression of these EMT-related genes was associated with poor survival in BCa (Figure S2).

### 3.4. Correlation of CYTOR expression with immune cell infiltration in BCa

This finding suggests that *CYTOR* is related to immune-related pathways. Therefore, we explored the difference in immune cell infiltration of *CYTOR* in BCa. First, we used the ESTIMATE algorithm to calculate the stromal score and immune score of each BCa sample and observed lower immune scores ($p = 0.0086$, Fig. 4A) and higher stromal scores ($p = 0.0045$, Fig. 4B) in the *CYTOR* high-expressing group than in the *CYTOR* low-expressing group, indicating that the expression level of *CYTOR* could influence the infiltration level of stromal cells and immune cells in tumor tissues. We further analyzed the abundance of 22 tumor-infiltrating immune cells in the two groups and found that apart from Tregs ($p = 0.027$), the proportions of M2 macrophages ($p = 0.001$) were significantly increased in the *CYTOR* high-expressing group (Fig. 4C). In addition, *CYTOR* expression was positively associated with the expression of M2 polarization markers, including *CD163* (Fig. 4D), *MS4A4A* (Fig. 4E) and *VSIG4* (Fig. 4F). Survival analysis showed that patients with high M2 macrophage infiltration tended to have a poor prognosis ($p = 0.044$, Fig. 4G). Taken together, these results indicated that *CYTOR* overexpression may alter the M2 macrophages response, which influences tumor progression and promotes the malignant behavior of BCa. UTUC accounts for 5–10% of all urothelial cancers [20]. It is generally believed that UTUC and BCa are both urothelial carcinomas and share many similar characteristics [21]. In our UTUC transcriptome dataset, we also found that elevated *CYTOR* was associated with an increased proportion of M2 macrophages, which is consistent with the preceding analysis in the TCGA-BCa dataset ($p = 0.03$, Fig. 4H). Moreover, UTUC patients with high expression of *CYTOR* also showed a much worse prognosis ($p=0.039$, Fig. 4I).

**Table 1**
Correlation between *CYTOR* expression and clinicopathological features in BCa from TCGA.

| Features | *CYTOR* expression | | Pearson *x2* | P |
|---|---|---|---|---|
| | Low | High | | |
| Age (years), no (%) | | | | |
| ≤60 | 121 (59.9) | 108 (53.2) | | |
| >60 | 81 (40.1) | 95 (46.8) | 1.849 | 0.174 |
| Gender, no (%) | | | | |
| Male | 160 (79.2) | 140 (69.0) | | |
| Female | 42 (20.8) | 63 (31.0) | 5.531 | **0.019** |
| Pathologic stage, no (%) | | | | |
| I + II | 83 (41.1) | 50 (24.6) | | |
| III + IV | 119 (58.9) | 153 (75.4) | 12.436 | < **0.001** |
| Histologic grade, no (%) | | | | |
| Low | 18 (8.9) | 3 (1.5) | | |
| High | 182 (90.1) | 199 (98.0) | | |
| NA | 2 (1.0) | 1 (0.5) | 12.983 | **0.002** |
| Diagnosis subtype, no (%) | | | | |
| Non-Papillary | 117 (57.9) | 153 (75.4) | | |
| Papillary | 84 (41.6) | 47 (23.2) | | |
| NA | 1 (0.5) | 3 (1.5) | 16.452 | < **0.001** |

**Table 2**
Univariate and multivariate Cox regression analysis of *CYTOR* level with overall survival in BCa from TCGA.

| Features | Univariate COX | | Multivariate COX | |
|---|---|---|---|---|
| | HR (95% CI) | P | HR (95% CI) | P |
| Age (>60 vs ≤ 60) | 1.473 (1.097, 1.976) | **0.010** | 1.420 (1.047, 1.926) | **0.024** |
| Gender (Male vs Female) | 0.853 (0.616, 1.181) | 0.339 | | |
| Pathologic-T (T3-T4 vs T1-T2) | 1.469 (1.219, 1.771) | < **0.001** | 1.471 (1.220, 1.773) | < **0.001** |
| Histologic grade (High vs Low) | 1.053 (0.597, 1.857) | 0.858 | | |
| *CYTOR* level (High vs Low) | 1.380 (1.030, 1.86) | **0.033** | | |

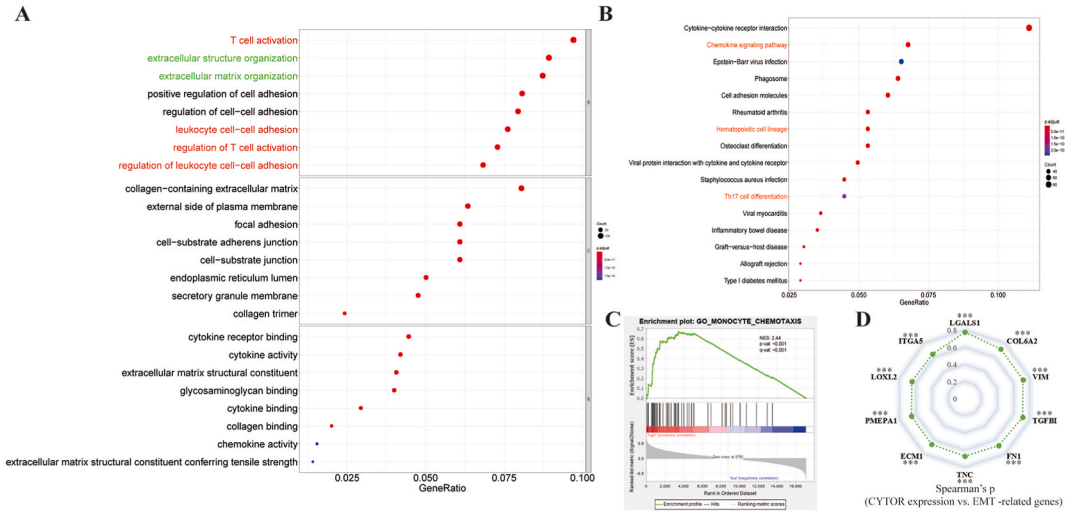


**Fig. 3.** Pathway enrichment analysis of *CYTOR* in BCa. (A) GO term and (B) KEGG enrichment analysis for genes co-expressed with *CYTOR* in BCa. (C) GSEA was performed according to the expression level of *CYTOR* in TCGA database. The median expression of *CYTOR* was selected as the cut-off value. (D) *CYTOR* expression levels are positively correlated with EMT-related genes expression levels. ***p < 0.001.

### 3.5. *CYTOR facilitates the crosstalk between CAFs and macrophages*

Previously, we found that elevated *CYTOR* expression was associated with an increased proportion of M2 macrophages. We next explored the role of *CYTOR* in the TME. Single-cell mRNA profiles of eight primary tumors and three normal samples from GSA-Human under accession code HRA000212 were obtained. After quality control and normalization of the raw data, we analyzed the expression of *CYTOR* in these samples and found that *CYTOR* expression was upregulated in the tumor samples (Fig. 5A). Then, we selected conventional markers to cluster and annotate the filtered cells into eight major clusters, including epithelial (tumor) cells, T/NK cells, endothelial cells, CAFs, B cells, macrophages, mast cells and monocytes (Fig. 5B–C). We first investigated the expression level of *CYTOR* in the eight cell types. Interestingly, we found that *CYTOR* expression was highest in CAFs rather than in macrophages (Fig. 5D). Furthermore, *CYTOR* expression was positively associated with the expression of CAF cell markers, including *COL1A1* ($r = 0.586$, $p < 0.001$), *COL1A2* ($r = 0.583$, $p < 0.001$), *COL3A1* ($r = 0.542$, $p < 0.001$), *SFRP2* ($r = 0.510$, $p < 0.001$), *DCN* ($r = 0.448$, $p < 0.001$) and *LUM* ($r = 0.456$, $p < 0.001$), in the TCGA-BCa dataset (Fig. 5E). To investigate the role of *CYTOR* in fibroblast-macrophage interactions, we applied CellChat (version 1.4.0), a tool that takes gene expression data from cells as the input and combines it with ligand–receptor and cofactor interactions to simulate intercellular communication [22]. We first divided the patients into two groups according to the expression of *CYTOR* in CAFs. Group A included patient 3, patient 6 and patient 8, all of whom were almost completely lacking *CYTOR* expression in fibroblasts, and Group B included five other patients who had high *CYTOR* expression in fibroblasts (Fig. 5F). Then, we investigated the communication strength between the two groups. We found fewer ligand–receptor pairs between CAFs and macrophages in Group A (Fig. 5G) than in Group B (Fig. 5H), implying stronger cellular communication between CAFs and macrophages in Group B. Moreover, the expression levels of M2 polarization markers (*CD163*, *MRC1*, *MS4A4A* and *VSIG4*) in macrophages were elevated in Group B compared to Group A (Fig. 5I). Taken together, our results reveal that high *CYTOR* expression in CAFs may enhance the crosstalk between CAFs and macrophages, thus mediating M2 polarization of macrophages.

### 3.6. *CYTOR may act as an indicator of the response to immunotherapy*

Immune checkpoint inhibitors, an emerging therapeutic modality, have shown promising results in the treatment of advanced bladder cancer, and evaluation of immune targets may serve as a predictor of immunotherapy efficacy. It was suggested that *CYTOR*

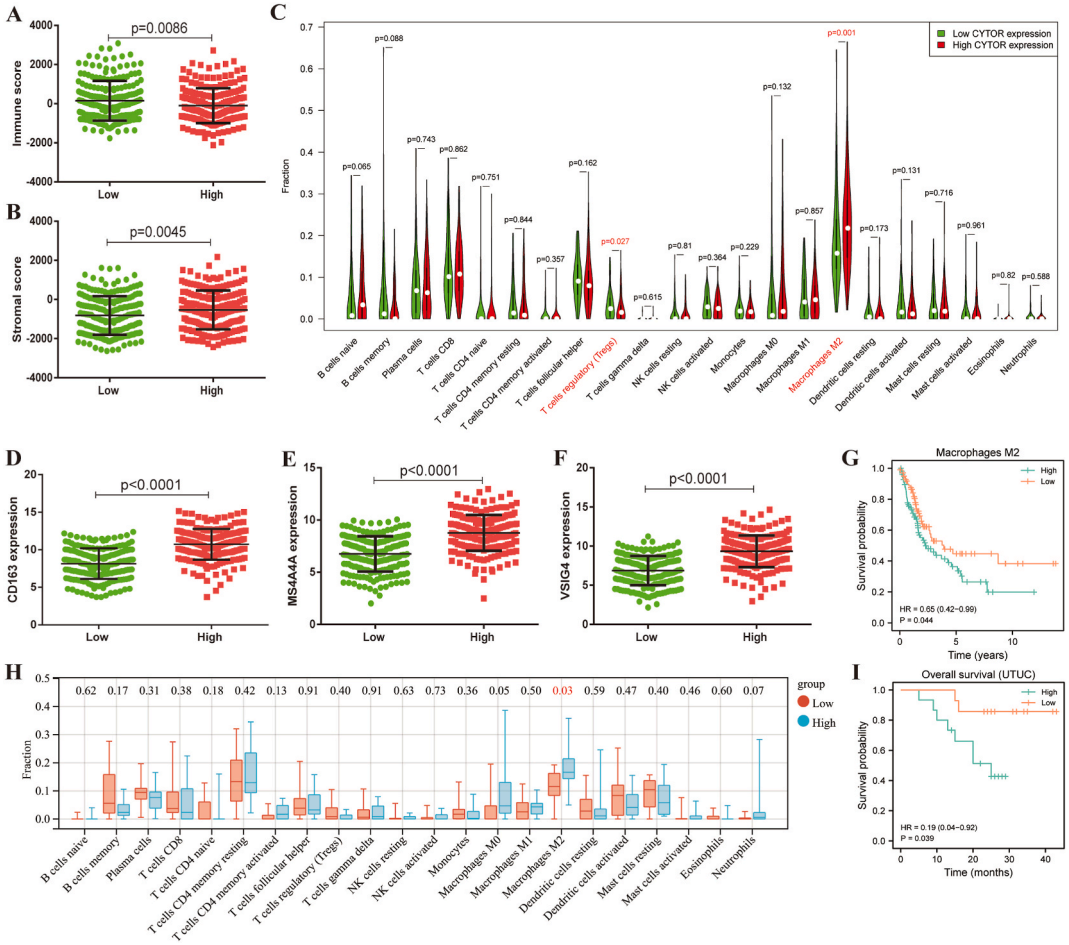


**Fig. 4.** Correlation of *CYTOR* expression with immune cell infiltration in BCa. (A) The immune score in the groups of high *CYTOR* expression and low *CYTOR* expression. (B) The stromal score in the groups of high *CYTOR* expression and low *CYTOR* expression. (C) The distribution of 22 tumor-infiltrating immune cells among different groups as defined by the expression of *CYTOR*. (D–F) The expression of *CD163* (D), *MS4A4A* (E) and *VSIG4* (F) in the groups of high *CYTOR* expression and low *CYTOR* expression. (G) Survival analysis of the abundance ratios of M2 macrophages. (H) The distribution of 22 tumor-infiltrating immune cells among different groups as defined by the expression of *CYTOR* in UTUC dataset. (I) Expression level of *CYTOR* was related to the prognosis of UTUC.

may be involved in immune-related pathways, so we explored the potential of *CYTOR* expression as an indicator of immunotherapy response. First, we evaluated the correlation between the expression of *CYTOR* and the expression levels of immune checkpoint genes. The results showed that *PD-1/PD-L1* expression in patients in the *CYTOR* high-expressing group was significantly higher than that in the *CYTOR* low-expressing group ($p = 0.0045$ and $p = 0.0086$, respectively) (Fig. 6A–B). Spearman correlation showed that *CYTOR* had a significant positive association with *PD-1* ($r = 0.503$, $p < 0.001$, Fig. 6C) and *PD-L1* ($r = 0.549$, $p < 0.001$, Fig. 6D) expression. Moreover, we also found that *CYTOR* had a positive expression correlation with other targets for specific immunotherapy, including *IDO1*, *PD-L2*, *CTLA-4* and *TIM-3* (Fig. 6E). Interestingly, the expression of *CYTOR* had a positive expression correlation with *PD-1* and *PD-L1* in 14 individual cancer types and in pancancer ($p < 0.05$) (Fig. 6F–G). These results suggest that *CYTOR* expression may be a positive predictor for *anti*-PD-1/PD-L1 immunotherapy.

### *3.7. Validation of CYTOR expression and correlation with the malignant phenotype of BCa*

We first compared *CYTOR* expression levels in a normal urothelial cell line and several different bladder cancer cell lines. Among the seven bladder cancer cell lines, six exhibited significant upregulation of *CYTOR* (Fig. 7A). We then analyzed relative *CYTOR* expression (tumor/adjacent control) in tumor samples from 24 patients with BCa. As shown in Fig. 7B, *CYTOR* expression was significantly elevated in 70.8% (17/24) of BCa tissues compared with normal urothelium. Next, these samples were divided into a *CYTOR* low-expressing group and a *CYTOR* high-expressing group according to the median value of *CYTOR* expression. Clinicopathological features, such as age (Fig. 7C), sex (Fig. 7D), TNM stage (Fig. 7E-H) and histological grade (Fig. 7I), were obtained and compared between the two groups. The results showed that high expression of *CYTOR* was associated with young age, male sex, higher

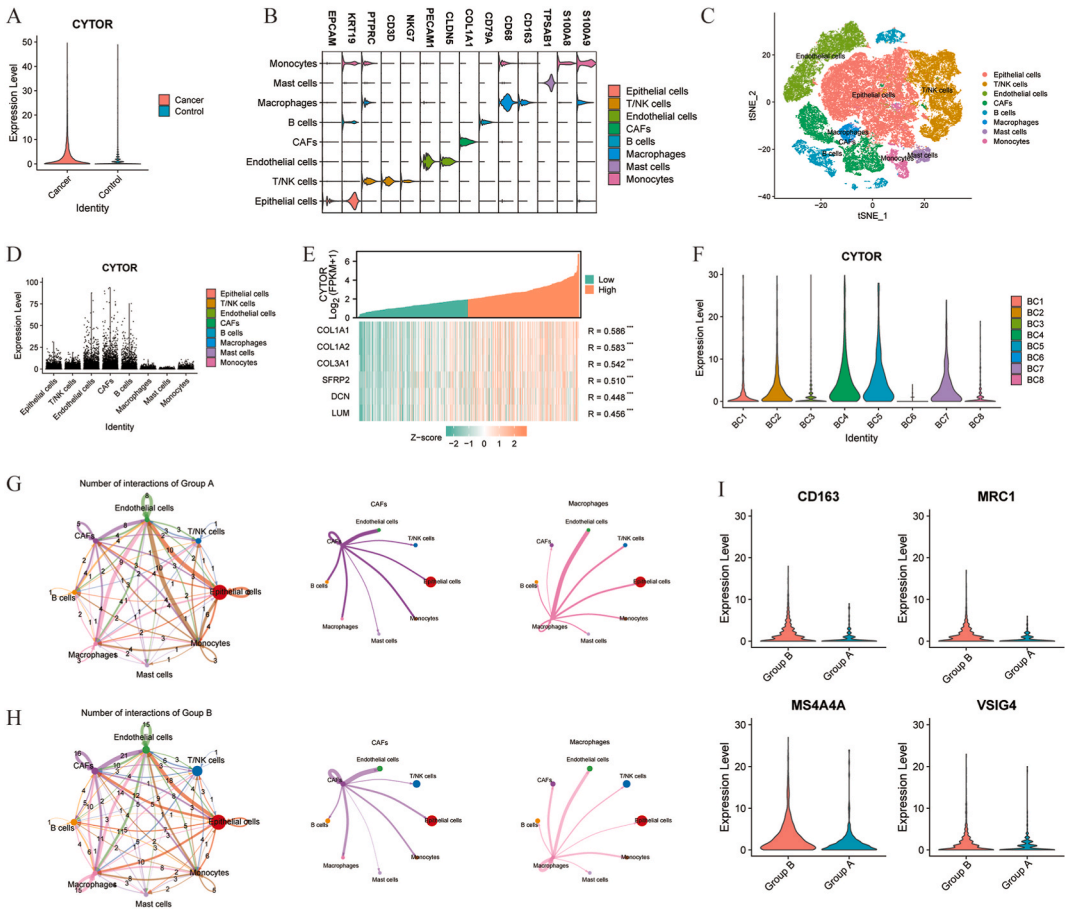


**Fig. 5.** *CYTOR* facilitates the cross-talk between CAFs and macrophages. (A) The mRNA level of *CYTOR* in the single cell dataset of BCa. (B) Violin plot showed the cell markers of epithelial (tumor) cells, T/NK cells, endothelial cells, CAFs, B cells, macrophages, mast cells and monocytes. (C) tSNE plot of single cells colored by major cell types. (D) The expression level of *CYTOR* in eight major cell clusters. (E) Heatmap showed the relationship between *CYTOR* and CAFs cell markers in the TCGA-BCa dataset. (F) The expression level of *CYTOR* in CAFs of eight BCa patients. (G) Cell-cell communication in Group A. The left picture showed the number of significant ligand-receptor pairs between any pair of two cell populations. The edge width is proportional to the predicted number of ligand-receptor pairs and represents the communication probability. The size of the circle is proportional to the number of cells in each cell group. The middle picture displayed putative ligand-receptor interactions between CAFs and other cell clusters. The right picture displayed putative ligand-receptor interactions between macrophages and other cell clusters. (H) Cell-cell communication in Group B. The left picture showed the number of significant ligand-receptor pairs between any pair of two cell populations. The middle picture displayed putative ligand-receptor interactions between CAFs and other cell clusters. The right picture displayed putative ligand-receptor interactions between macrophages and other cell clusters. (I) The expression levels of M2 polarization markers *(CD163*, *MRC1*, *MS4A4A* and *VSIG4*) in macrophages of Group A and Group B.

TNM stage, advanced pathologic stage and advanced histologic grade, which was largely consistent with the results of previous analysis. *CYTOR* expression in patients of different sexes was inconsistent with TCGA analysis, which may be due to analysis bias caused by the small sample size. We next examined the effects of *CYTOR* on the migration and invasion ability of bladder cancer cells. Lentivirus-mediated knockdown of *CYTOR* in T24 cells was performed and the knockdown efficiency was subsequently measured by RT-qPCR ($p < 0.01$, Fig. 7J). Compared with the migration of sh-NC groups, the migratory capacity of the T24 sh-*CYTOR* groups were significantly inhibited after 24 h ($p < 0.01$, Fig. 7K). Cell invasion was also strongly inhibited in the T24 sh-*CYTOR* groups ($p < 0.01$, Fig. 7K). Furthermore, we confirmed the effects of *CYTOR* on tumor growth. By injecting T24/sh-*CYTOR* and T24/sh-NC cells into nude mice, we generated the sh-*CYTOR* and sh-NC groups. The growth of tumors was slower in the sh-*CYTOR* group than in the sh-NC group. Mice were sacrificed on the 60th day after injection, and the tumor tissue was collected. Tumors from the sh-NC group were larger and heavier than those from the sh-*CYTOR* group ($p < 0.05$, Fig. 7L–M).

## 4. Discussion

*CYTOR* is a lncRNA that is differentially expressed in a variety of tumors. Recent studies have shown that *CYTOR* is associated with patient prognosis and that high *CYTOR* expression in most tumors predicts poor clinical outcome [23–26]. For example, in

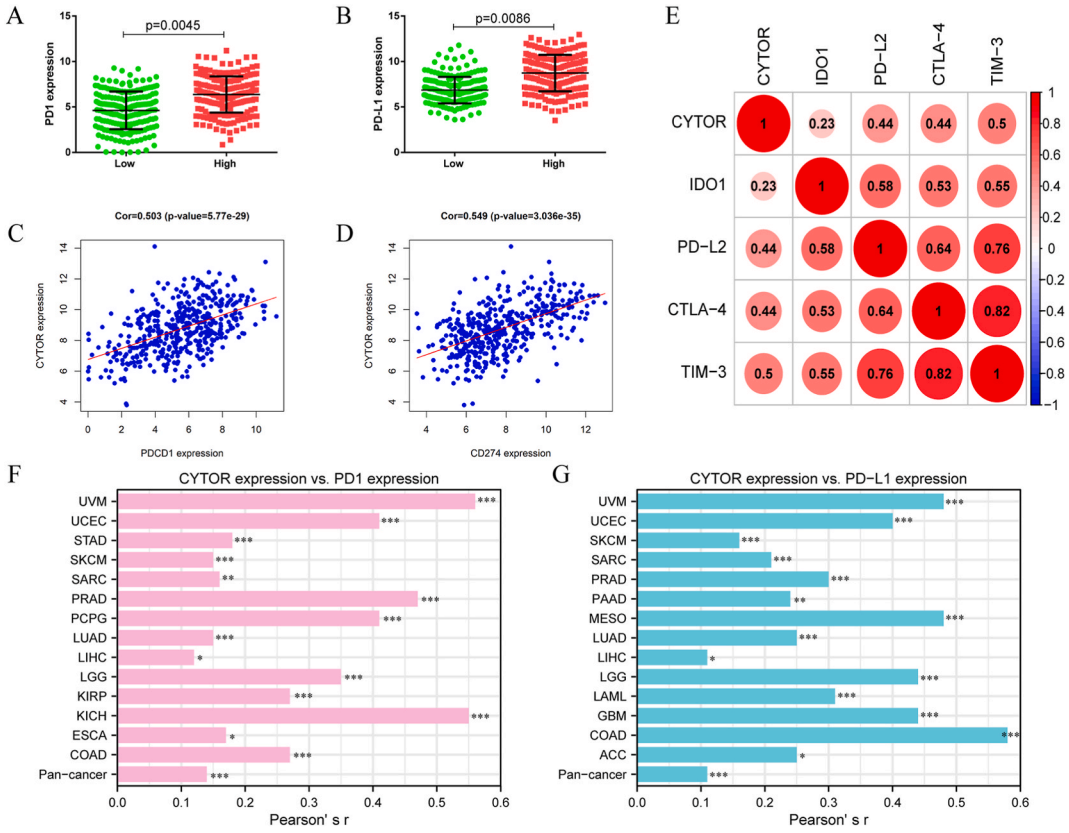


**Fig. 6.** *CYTOR* could serve as a predictive marker for immunotherapy. (A–B) The expression of *PD-1* (A) and *PD-L1* (B) in the groups of BCa with high *CYTOR* expression and low *CYTOR* expression. (*C*–D) Significant association between *CYTOR* and the immune checkpoint inhibitors *PD-1* (C) and *PD-L1* (D) in BCa. (E) The relationship between *CYTOR* and immune checkpoint genes in BCa. (F) The positive expression correlation between *CYTOR* and *PD-1* across cancers. (G) The positive expression correlation between *CYTOR* and *PD-L1* across cancers. *p < 0.05, **p < 0.01, ***p < 0.001.

hepatocellular carcinoma, *CYTOR* affects the proliferation, cell cycle and apoptosis of hepatocellular carcinoma cells by regulating the miR-125b-5p/KIAA1522 axis [27]. In colon cancer, *CYTOR* conferred resistance to oxaliplatin-induced apoptosis and promoted metastasis [28]. Additionally, *CYTOR* promoted lung adenocarcinoma proliferation by interacting with EZH2 and repressing IL24 expression [29,30]. Nevertheless, the role of *CYTOR* in BCa remains to be elucidated.

In our study, we first compared the expression of *CYTOR* in 33 tumor types and corresponding normal samples. Differential expression of *CYTOR* was found in 18 distinct tumor types, and most (17/18) of them exhibited an increase in tumor samples. Survival analysis revealed that increased expression of *CYTOR* was associated with a worse prognosis of tumor patients, which implied that *CYTOR* may be an oncogene in most tumors. The predictive value of lncRNAs for BCa in terms of prognosis and response to treatment has been widely evaluated and reported [6,31]. We then analyzed the correlation between *CYTOR* expression and clinicopathological features of BCa and found that *CYTOR* was significantly elevated in BCa compared to adjacent normal tissue. In addition, elevated *CYTOR* expression predicted worse prognosis, higher pathologic T stage, advanced histological grade and a greater propensity for local recurrence, indicating that *CYTOR* has potential application value in predicting survival and recurrence of BCa. However, multivariate analysis showed that *CYTOR* expression was not an independent risk factor for OS in BCa patients. This result may be caused by the limited sample size.

To explore the biological function of *CYTOR* in BCa, enrichment analysis revealed a possible role of *CYTOR* in BCa by inducing immune-related pathways and EMT. Further analysis of immune infiltration revealed that *CYTOR* may alter the Treg and M2 macrophage response; Tregs and M2 macrophages populate the microenvironment of solid tumors and promote tumor progression of BCa [32,33]. Interestingly, we observed that *CYTOR* was mainly expressed in CAFs through scRNA-Seq analysis. Moreover, the expression level of *CYTOR* was positively correlated with the expression levels of *CD163*, *MRC1*, *MS4A4A* and *VSIG4*, which have been reported to promote the M2 polarization of macrophages [34–36]. CAFs are the most essential stromal components of the TME, and activated CAFs can promote tumor growth, invasion and metastasis, along with extracellular matrix remodeling and even chemoresistance [37,38]. Current studies have confirmed that CAFs interact with many immune components within the TME and shape an immunosuppressive TME, including restricting the recruitment of immune effector cells and facilitating the recruitment of inhibitory immune cells [37]. However, the interaction of CAFs with macrophages in BCa has rarely been reported. Our study revealed that high

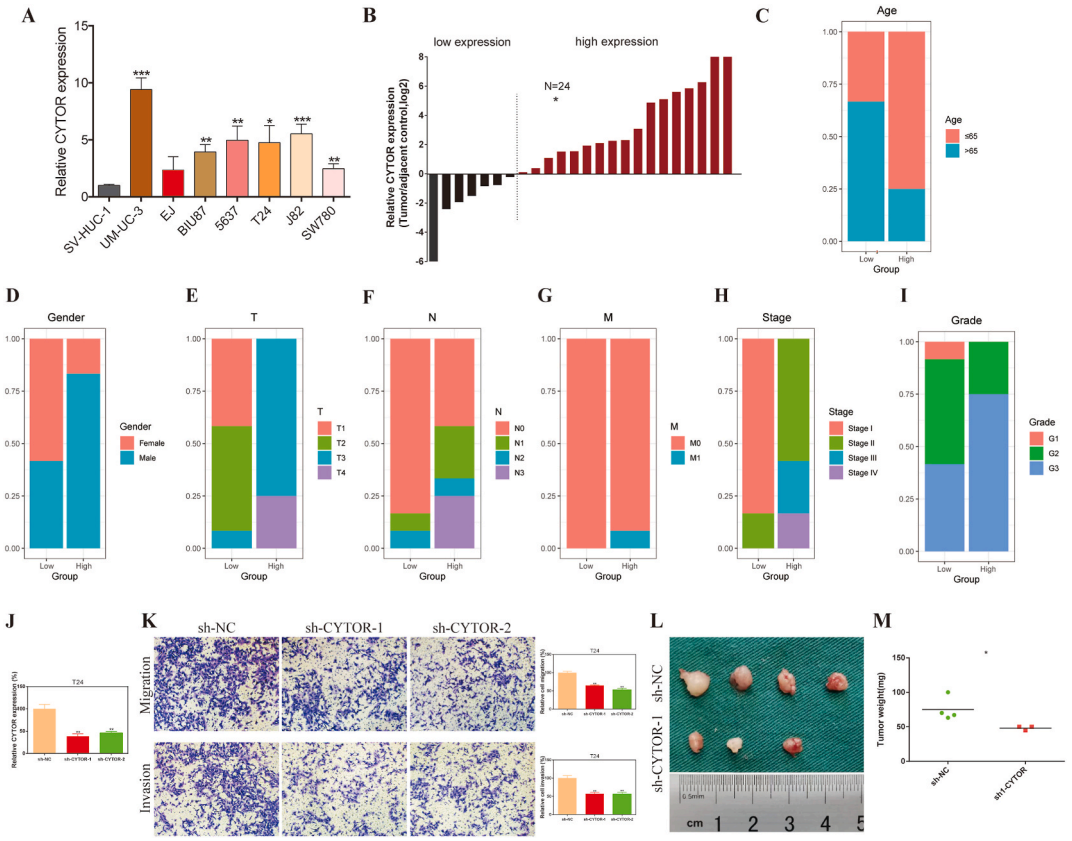


**Fig. 7.** Validation of *CYTOR* expression and correlation with malignant phenotype of BCa. (A) *CYTOR* mRNA expression in BCa cell lines compared with normal urothelial SV-HUC-1 cells. (B) *CYTOR* mRNA expression in BCa tissues compared with adjacent normal urothelium. (*C*–I) High *CYTOR* expression was related to young patients (C), male (D), higher pathologic T stage (E), higher pathologic N stage (F), higher pathologic M stage (G), advanced pathologic stage (H) and advanced histologic grade (I). (J) RT-qPCR analyses of T24 cells infected with a *CYTOR* shRNA vector. (K) Representative images of transwell migration and invasion assay of T24-sh-*CYTOR* cells. (L) Tumors collected from nude mice injected with T24-sh-*CYTOR* cells are shown. (M) Tumor weights of the sh-*CYTOR* and sh-NC treatment groups were measured. *p < 0.05, **p < 0.01, ***p < 0.001.

*CYTOR* expression in CAFs may facilitate crosstalk between CAFs and macrophages, thereby promoting an M2 phenotype and BCa progression.

Due to the high risk of recurrence after radical surgery for MIBC and the significant toxic side effects of traditional neoadjuvant chemotherapy regimens, a significant proportion of patients are ineligible for cisplatin chemotherapy. With the advent of immunotherapy, PD-1/PD-L1 inhibitors have demonstrated the potential to achieve durable objective responses in BCa [39]. However, only 23% of patients with advanced BCa respond to immunotherapy [40]. Therefore, exploring more effective targets to predict the response to immunotherapy has gradually become a hot topic in immunology. The expression of immune checkpoint genes, such as *PD-1* and *PD-L1*, has been confirmed to be an indicator of immunotherapy response [41,42]. Currently, lncRNAs with predictive value for immunotherapy response in BCa continue to be identified and reported [43–45]. With the continuous discovery of more immune-related lncRNAs, suitable patients can be screened more effectively, thereby improving the overall response rate of immunotherapy for BCa. In our study, the correlation analysis showed that *CYTOR* was positively related to *PD-1/PD-L1* and other targets for specific immunotherapies, suggesting its application value in predicting the efficacy of immunotherapy. However, there remained some limitations of our research including the lack of biological experiment to prove that *CYTOR* may influence the tumor microenvironment and increase the immunotherapy response of BCa.

## 5. Conclusions

In conclusion, we identified *CYTOR* as a cancer immune-related lncRNA, that has not been reported previously. Our work suggests that *CYTOR* may influence the tumor microenvironment, promote tumor progression and increase the immunotherapy response of BCa. To confirm the relationship between *CYTOR* and immune infiltration, further experiments are needed.

## Ethics approval and consent to participate

Written informed consent was obtained from all patients prior to sample collection. This study was approved by the Biomedical Research Ethics Committee of Peking University First Hospital [approval number: 2015 (977)].

## Consent for publication

Not applicable.

## Author contribution statement

Yucai Wu: Performed the experiments; Analyzed and interpreted the data; Wrote the paper.
Yangyang Xu; Jian Fan: Analyzed and interpreted the data.
Shiming He; Yifan Li: Contributed reagents, materials, analysis tools or data.
Ninghan Feng; Yanqing Gong; Xuesong Li; Liqun Zhou: Conceived and designed the experiments.

## Funding statement

This work was supported by the National Key R&D Program of China [2019YFA0906001], National Natural Science Foundation of China [81772703, 82070704, 82002675 and 81972380], Wuxi "Taihu Talents Program" Medical and Health High-level Talents Project, National High Level Hospital Clinical Research Funding (Scientific Research Seed Fund of Peking University First Hospital) [2022SF18], Clinical Medicine Plus X -Young Scholars Project of Peking University [PKU2021LCXQ026], and Jiangsu Natural Science Research of Colleges and Universities-General Project [20KJB320014].

## Data availability statement

Data will be made available on request.

## Declaration of interest's statement

The authors declare that they have no known competing financial interests or personal relationships that could have appeared to influence the work reported in this paper.

## Acknowledgements

None.

## Appendix A. Supplementary data

Supplementary data to this article can be found online at https://doi.org/10.1016/j.heliyon.2023.e13707.

## References

[1] F. Bray, J. Ferlay, I. Soerjomataram, R.L. Siegel, L.A. Torre, A. Jemal, Global cancer statistics 2018: GLOBOCAN estimates of incidence and mortality worldwide for 36 cancers in 185 countries, CA A Cancer J. Clin. 68 (2018) 394–424.
[2] V.G. Patel, W.K. Oh, M.D. Galsky, Treatment of muscle-invasive and advanced bladder cancer in 2020, CA A Cancer J. Clin. 70 (2020) 404–423.
[3] C.P. Ponting, P.L. Oliver, W. Reik, Evolution and functions of long noncoding RNAs, Cell 136 (2009) 629–641.
[4] J. Zhao, Y. Liu, W. Zhang, Z. Zhou, J. Wu, P. Cui, Y. Zhang, G. Huang, Long non-coding RNA Linc00152 is involved in cell cycle arrest, apoptosis, epithelial to mesenchymal transition, cell migration and invasion in gastric cancer, Cell Cycle 14 (2015) 3112–3123.
[5] G.J. Goodall, V.O. Wickramasinghe, RNA in cancer, Nat. Rev. Cancer 21 (2021) 22–36.
[6] X. Chen, R. Xie, P. Gu, M. Huang, J. Han, W. Dong, W. Xie, B. Wang, W. He, G. Zhong, Z. Chen, J. Huang, T. Lin, Long noncoding RNA LBCS inhibits self-renewal and chemoresistance of bladder cancer stem cells through epigenetic silencing of SOX2, Clin. Cancer Res. 25 (2019) 1389–1403.
[7] Z. Chen, X. Chen, R. Xie, M. Huang, W. Dong, J. Han, J. Zhang, Q. Zhou, H. Li, J. Huang, T. Lin, DANCR promotes metastasis and proliferation in bladder cancer cells by enhancing IL-11-STAT3 signaling and CCND1 expression, Mol. Ther. 27 (2019) 326–341.
[8] Q. Hu, Y. Ye, L.C. Chan, Y. Li, K. Liang, A. Lin, S.D. Egranov, Y. Zhang, W. Xia, J. Gong, Y. Pan, S.S. Chatterjee, J. Yao, et al., Oncogenic lncRNA downregulates cancer cell antigen presentation and intrinsic tumor suppression, Nat. Immunol. 20 (2019) 835–851.
[9] L. Zhao, Y. Liu, J. Zhang, Y. Liu, Q. Qi, LncRNA SNHG14/miR-5590-3p/ZEB1 positive feedback loop promoted diffuse large B cell lymphoma progression and immune evasion through regulating PD-1/PD-L1 checkpoint, Cell Death Dis. 10 (2019) 731.
[10] D. Huang, J. Chen, L. Yang, Q. Ouyang, J. Li, L. Lao, J. Zhao, J. Liu, Y. Lu, Y. Xing, F. Chen, F. Su, H. Yao, et al., NKILA lncRNA promotes tumor immune evasion by sensitizing T cells to activation-induced cell death, Nat. Immunol. 19 (2018) 1112–1125.
[11] B. Yue, D. Cai, C. Liu, C. Fang, D. Yan, Linc00152 functions as a competing endogenous RNA to confer oxaliplatin resistance and holds prognostic values in colon cancer, Mol. Ther. 24 (2016) 2064–2077.

[12] Y. Wu, C. Tan, W.W. Weng, Y. Deng, Q.Y. Zhang, X.Q. Yang, H.L. Gan, T. Wang, P.P. Zhang, M.D. Xu, Y.Q. Wang, C.F. Wang, Long non-coding RNA Linc00152 is a positive prognostic factor for and demonstrates malignant biological behavior in clear cell renal cell carcinoma, Am J Cancer Res 6 (2016) 285–299.
[13] Q. Cai, Z.Q. Wang, S.H. Wang, C. Li, Z.G. Zhu, Z.W. Quan, W.J. Zhang, Upregulation of long non-coding RNA LINC00152 by SP1 contributes to gallbladder cancer cell growth and tumor metastasis via PI3K/AKT pathway, Am J Transl Res 8 (2016) 4068–4081.
[14] J. Liang, X. Wei, Z. Liu, D. Cao, Y. Tang, Z. Zou, C. Zhou, Y. Lu, Long noncoding RNA CYTOR in cancer: a TCGA data review, Clin. Chim. Acta 483 (2018) 227–233.
[15] K. Yoshihara, M. Shahmoradgoli, E. Martínez, R. Vegesna, H. Kim, W. Torres-Garcia, V. Treviño, H. Shen, P.W. Laird, D.A. Levine, S.L. Carter, G. Getz, K. Stemke-Hale, et al., Inferring tumour purity and stromal and immune cell admixture from expression data, Nat. Commun. 4 (2013) 2612.
[16] A. Subramanian, H. Kuehn, J. Gould, P. Tamayo, J.P. Mesirov, GSEA-P: a desktop application for gene set enrichment analysis, Bioinformatics 23 (2007) 3251–3253.
[17] A.M. Newman, C.L. Liu, M.R. Green, A.J. Gentles, W. Feng, Y. Xu, C.D. Hoang, M. Diehn, A.A. Alizadeh, Robust enumeration of cell subsets from tissue expression profiles, Nat. Methods 12 (2015) 453–457.
[18] Y. Wu, Y. Peng, B. Guan, A. He, K. Yang, S. He, Y. Gong, X. Li, L. Zhou, P4HB: a novel diagnostic and prognostic biomarker for bladder carcinoma, Oncol. Lett. 21 (2021) 95.
[19] T. Li, J. Fu, Z. Zeng, D. Cohen, J. Li, Q. Chen, B. Li, X.S. Liu, TIMER2.0 for analysis of tumor-infiltrating immune cells, Nucleic Acids Res. 48 (2020) W509–W514.
[20] M. Rouprêt, M. Babjuk, M. Burger, O. Capoun, D. Cohen, E.M. Compérat, N.C. Cowan, J.L. Dominguez-Escrig, P. Gontero, A. Hugh Mostafid, J. Palou, B. Peyronnet, T. Seisen, et al., European association of Urology Guidelines on upper urinary tract urothelial carcinoma: 2020 update, Eur. Urol. 79 (2021) 62–79.
[21] D.A. Green, M. Rink, E. Xylinas, S.F. Matin, A. Stenzl, M. Roupret, P.I. Karakiewicz, D.S. Scherr, S.F. Shariat, Urothelial carcinoma of the bladder and the upper tract: disparate twins, J. Urol. 189 (2013) 1214–1221.
[22] S. Jin, C.F. Guerrero-Juarez, L. Zhang, I. Chang, R. Ramos, C.H. Kuan, P. Myung, M.V. Plikus, Q. Nie, Inference and analysis of cell-cell communication using CellChat, Nat. Commun. 12 (2021) 1088.
[23] S. Wang, W. Weng, T. Chen, M. Xu, P. Wei, J. Li, L. Lu, Y. Wang, LINC00152 promotes tumor progression and predicts poor prognosis by stabilizing BCL6 from degradation in the epithelial ovarian cancer, Front. Oncol. 10 (2020), 555132.
[24] B.J. Reon, B.T.R. Karia, M. Kiran, A. Dutta, LINC00152 promotes invasion through a 3 '-Hairpin structure and associates with prognosis in glioblastoma, Mol. Cancer Res. 16 (2018) 1470–1482.
[25] P.P. Zhang, Y.Q. Wang, W.W. Weng, W. Nie, Y. Wu, Y. Deng, P. Wei, M.D. Xu, C.F. Wang, Linc00152 promotes cancer cell proliferation and invasion and predicts poor prognosis in lung adenocarcinoma, J. Cancer 8 (2017) 2042–2050.
[26] J. Yu, Y. Liu, C. Guo, S. Zhang, Z. Gong, Y. Tang, L. Yang, Y. He, Y. Lian, X. Li, H. Deng, Q. Liao, X. Li, et al., Upregulated long non-coding RNA LINC00152 expression is associated with progression and poor prognosis of tongue squamous cell carcinoma, J. Cancer 8 (2017) 523–530.
[27] B. Hu, X.B. Yang, X. Yang, X.T. Sang, LncRNA CYTOR Affects the Proliferation, Cell Cycle and Apoptosis of Hepatocellular Carcinoma Cells by Regulating the miR-125b-5p/KIAA1522 axis, vol. 12, Aging, Albany NY), 2020.
[28] B. Yue, C. Liu, H. Sun, M. Liu, C. Song, R. Cui, S. Qiu, M. Zhong, A positive feed-forward loop between LncRNA-CYTOR and wnt/beta-catenin signaling promotes metastasis of colon cancer, Mol. Ther. 26 (2018) 1287–1298.
[29] Q.N. Chen, X. Chen, Z.Y. Chen, F.Q. Nie, C.C. Wei, H.W. Ma, L. Wan, S. Yan, S.N. Ren, Z.X. Wang, Long intergenic non-coding RNA 00152 promotes lung adenocarcinoma proliferation via interacting with EZH2 and repressing IL24 expression, Mol. Cancer 16 (2017) 17.
[30] S.M. Feng, J. Zhang, W.M. Su, S.B. Bai, L. Xiao, Z.W. Wang, J. Lin, R. Reddy, A. Chang, D. Beer, G.A. Chen, LINC00152 regulates cell proliferation via p38 signaling and overexpression predicts poor patient survival in lung cancer, Cancer Res. (2017) 77.
[31] Z. Sun, C. Jing, C. Xiao, T. Li, An autophagy-related long non-coding RNA prognostic signature accurately predicts survival outcomes in bladder urothelial carcinoma patients, Aging (Albany NY) 12 (2020) 15624–15637.
[32] M. Huang, W. Dong, R. Xie, J. Wu, Q. Su, W. Li, K. Yao, Y. Chen, Q. Zhou, Q. Zhang, W. Li, L. Cheng, S. Peng, et al., HSF1 facilitates the multistep process of lymphatic metastasis in bladder cancer via a novel PRMT5-WDR5-dependent transcriptional program, Cancer Commun. 42 (2022) 447–470.
[33] T. Wang, Q. Zhou, H. Zeng, H. Zhang, Z. Liu, J. Shao, Z. Wang, Y. Xiong, J. Wang, Q. Bai, Y. Xia, Y. Wang, L. Liu, et al., CCR8 blockade primes anti-tumor immunity through intratumoral regulatory T cells destabilization in muscle-invasive bladder cancer, Cancer Immunol. Immunother. 69 (2020) 1855–1867.
[34] P.S. Zeiner, C. Preusse, A. Golebiewska, J. Zinke, A. Iriondo, A. Muller, T. Kaoma, K. Filipski, M. Müller-Eschner, S. Bernatz, A.E. Blank, P. Baumgarten, E. Ilina, et al., Distribution and prognostic impact of microglia/macrophage subpopulations in gliomas, Brain Pathol. 29 (2019) 513–529.
[35] I. Mattiola, F. Tomay, M. De Pizzol, R. Silva-Gomes, B. Savino, T. Gulic, A. Doni, S. Lonardi, M. Astrid Boutet, A. Nerviani, R. Carriero, M. Molgora, M. Stravalaci, et al., The macrophage tetraspan MS4A4A enhances dectin-1-dependent NK cell-mediated resistance to metastasis, Nat. Immunol. 20 (2019) 1012–1022.
[36] D. Zhang, X. Shen, K. Pang, Z. Yang, A. Yu, VSIG4 alleviates intracerebral hemorrhage induced brain injury by suppressing TLR4-regulated inflammatory response, Brain Res. Bull. 176 (2021) 67–75.
[37] X. Mao, J. Xu, W. Wang, C. Liang, J. Hua, J. Liu, B. Zhang, Q. Meng, X. Yu, S. Shi, Crosstalk between cancer-associated fibroblasts and immune cells in the tumor microenvironment: new findings and future perspectives, Mol. Cancer 20 (2021) 131.
[38] D. Dong, Y. Yao, J. Song, L. Sun, G. Zhang, Cancer-associated fibroblasts regulate bladder cancer invasion and metabolic phenotypes through autophagy, Dis. Markers 2021 (2021), 6645220.
[39] N. Lobo, C. Mount, K. Omar, R. Nair, R. Thurairaja, M.S. Khan, Landmarks in the treatment of muscle-invasive bladder cancer, Nat. Rev. Urol. 14 (2017) 565–574.
[40] A.V. Balar, M.D. Galsky, J.E. Rosenberg, T. Powles, D.P. Petrylak, J. Bellmunt, Y. Loriot, A. Necchi, J. Hoffman-Censits, J.L. Perez-Gracia, N.A. Dawson, M.S. van der Heijden, R. Dreicer, et al., Atezolizumab as first-line treatment in cisplatin-ineligible patients with locally advanced and metastatic urothelial carcinoma: a single-arm, multicentre, phase 2 trial, Lancet 389 (2017) 67–76.
[41] J.J. Havel, D. Chowell, T.A. Chan, The evolving landscape of biomarkers for checkpoint inhibitor immunotherapy, Nat. Rev. Cancer 19 (2019) 133–150.
[42] N. van Dijk, S.A. Funt, C.U. Blank, T. Powles, J.E. Rosenberg, M.S. van der Heijden, The cancer immunogram as a framework for personalized immunotherapy in urothelial cancer, Eur. Urol. 75 (2019) 435–444.
[43] R. Cao, L. Yuan, B. Ma, G. Wang, Y. Tian, Immune-related long non-coding RNA signature identified prognosis and immunotherapeutic efficiency in bladder cancer (BLCA), Cancer Cell Int. 20 (2020) 276.
[44] Y. Wu, L. Zhang, S. He, B. Guan, A. He, K. Yang, Y. Gong, X. Li, L. Zhou, Identification of immune-related LncRNA for predicting prognosis and immunotherapeutic response in bladder cancer, Aging (Albany NY) 12 (2020) 23306–23325.
[45] Y. Yu, W. Zhang, A. Li, Y. Chen, Q. Ou, Z. He, Y. Zhang, R. Liu, H. Yao, E. Song, Association of long noncoding RNA biomarkers with clinical immune subtype and prediction of immunotherapy response in patients with cancer, JAMA Netw. Open 3 (2020), e202149.